PERGAMON

Vision Research 38 (1998) 3913–3926

Vision Research

Chromatic masking in the (ΔL/L, ΔM/M) plane of cone-contrast space reveals only two detection mechanisms

Franco Giulianini, Rhea T. Eskew Jr*

Department of Psychology, 125 Nightingale Hall, Northeastern University, Boston, MA 02115, USA

Received 16 January 1997; received in revised form 13 November 1997

Abstract

The post-receptoral mechanisms that mediate detection of stimuli in the (ΔL/L, ΔM/M) plane of color space were characterized using noise masking. Chromatic masking noises of different chromaticities and spatial configurations were used, and threshold contours for the detection of Gaussian and Gabor tests were measured. The results do not show masking that is narrowly-selective for the chromaticity of the noise. On the contrary, our findings suggest that detection of these tests is mediated only by an opponent chromatic mechanism (a red-green mechanism) and a non-opponent luminance mechanism. These results are not consistent with the hypothesis of multiple chromatic mechanisms mediating detection in this color plane [1].

Keywords: Chromatic masking; Chromatic detection; Opponent mechanism; Higher order chromatic mechanism

1. Introduction

Results of psychophysical chromatic detection experiments have often been interpreted in terms of an opponent red-green (RG) detection mechanism that approximately equally weights the L- and M-cone contrast inputs, together with an opponent yellow-blue (YB) detection mechanism and a non-opponent luminance mechanism [2–9]. This classical notion of a visual system that encodes the visual information along two distinct chromatic dimensions plus a single achromatic one has been recently challenged by psychophysical studies reporting evidence for chromatic mechanisms sensitive to specific hues, such as, for example, orange or pink [1,10–13]. The evidence for these 'higher order' color mechanisms comes from both threshold [1,11,12] and suprathreshold experiments [10,13].

Krauskopf et al. [11,12] used a habituation paradigm to determine the cardinal directions of color space (stimuli along these directions are detected by distinct post-receptoral mechanisms). The stimuli were large chromatic fields; detection thresholds were measured before and after exposure to modulation of chromaticity along the cardinal axes and intermediate directions. In 1986 they reported that, in the equiluminant plane, thresholds were elevated most for tests that had the same chromaticity as the habituation stimuli, consistent with the presence of detection mechanisms that are tuned to specific hues in that plane. Krauskopf et al. referred to these mechanisms as 'higher-order color mechanisms' because they could be thought of as the result of a recombination of the signals generated by the classical mechanisms.

More recently, Gegenfurtner and Kiper [1], by measuring threshold elevation of Gabor patches in a noise masking procedure, found evidence for the existence of a multitude of chromatic mechanisms that are narrowly tuned to different directions in the (L, M) plane. However, when the stimuli used were simple square patches, they reported limited evidence for only two detection mechanisms. This result led them to speculate that stimuli containing a dc (non-zero spatial average) component might not be able to tap the activity of the narrowly-tuned mechanisms.

The purpose of the present study is to further investigate the existence of multiple, narrowly-tuned, chromatic mechanisms at threshold. Thresholds for the detection of localized patterns that modulate the activ-

* Corresponding author. Fax: +1 617 3738714; e-mail: eskew@neu.edu.

0042-6989/98/$19.00
PII: S0042-6989(98)00068-6

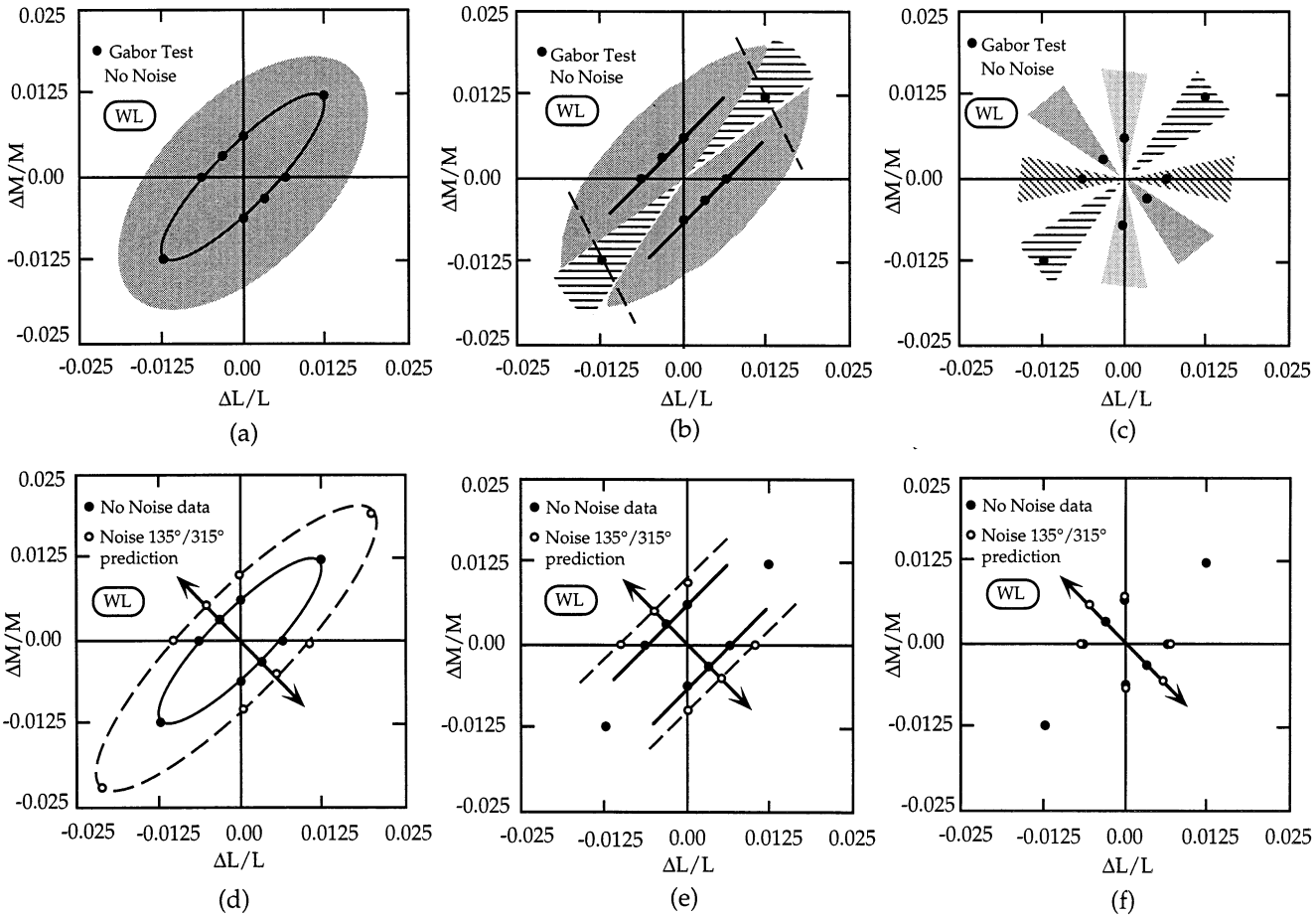

Fig. 1. Three interpretations of detection data (filled symbols): (a) as the result of the activity of a single line-element mechanism, (b) as the activity of two linear mechanisms, and (c) as the activity of many narrowly-tuned mechanisms. Panels (d–f) illustrate the predictions of each model after adding masking noise along the 135°/315° direction (black arrows). A single mechanism model predicts an expansion of the elliptical contour (d), a model based on only two mechanisms predicts a parallel shift of the two straight lines and little elevation for the test at 45° (e), and a model based on narrowly-tuned mechanisms predicts a distortion of the threshold contour around the 135°/315° direction (f). Data (filled symbols) are the no-noise thresholds of Fig. 7b.

ity of only the L- and M-cones were measured in the absence and presence of chromatic masking noise. We used two kinds of stimuli: simple Gaussian blobs (non-zero dc component) and Gabor patches in sine phase (zero dc component). The data are represented in the ($\Delta L/L$, $\Delta M/M$) plane of cone-contrast space.

Fig. 1 introduces the rationale of the experiments. The filled circles represent thresholds for the detection of Gabor patches at different angles in the ($\Delta L/L$, $\Delta M/M$) plane of cone contrast space for one of our observers (from Fig. 7b, below), together with some potential interpretations. One possible interpretation comes from the fact that all the thresholds could be very well fit by a single ellipse with high eccentricity (Fig. 1a). This would be consistent with detection mediated by a single detection mechanism that non-linearly combines the cone contrast inputs (a line-element model). Another possibility is to think of almost all the thresholds as aligned along two straight lines with slope of $+1$ and symmetric around the $\Delta L/L = \Delta M/M$ line (Fig. 1b). The equations for the two lines are $\Delta L/L - \Delta M/M = \pm K$, suggesting the activity of a single linear opponent detection mechanism that is sensitive to the difference of the L- and M-cone contrasts and that is responsible for the detection of almost all the tests. The opponent nature of this mechanism implies that it cannot respond to stimuli that generate approximately equal increments (or decrements) of the L- and M-cone contrasts (stimuli near the 45°/225° direction). These stimuli are presumably detected by a second mechanism (a non-opponent, luminance, mechanism with a threshold contour represented by the dashed lines). A third possibility is that these stimuli are detected by several chromatic mechanisms, each with a narrow spectrum of activity (Fig. 1c). According to this hypothesis, each of these mechanisms would be responsi-

ble for the detection of only those stimuli that lie within the region of the chromatic space to which they are sensitive, and the threshold contour is an envelope of their activities. This would be the kind of interpretation that the findings of Gegenfurtner and Kiper [1] support (at least for Gabor patches).

The main purpose of this study was to test these three possibilities using noise masking. For example, Fig. 1(d, e and f) shows the predictions made by the three different models when chromatic masking noise that varies along the 135°/315°, $\Delta L/L = -\Delta M/M$ direction is added to the Gabor tests (see Section 2). If detection were mediated by a single mechanism (Fig. 1a and d)—a model that has been repeatedly disproved in other contexts—the noise would affect all the thresholds equally and the ellipse would expand. If, on the other hand, detection in this plane were mediated by two mechanisms (Fig. 1b and e) the opponent mechanism would be strongly masked by this noise but the non-opponent mechanism would be much less masked: the two straight lines would move outward with no change in slope, while test thresholds at 45 and 225° would be relatively unaffected. Finally, if detection were mediated by several narrowly-tuned higher-order mechanisms (Fig. 1c and f), the noise would only affect mechanisms tuned to nearby directions, and the threshold contour would be distorted near the noise direction.

A fourth possibility is that the stimuli might be detected by several broadly-tuned (linear) higher-order chromatic mechanisms that are maximally sensitive to many different directions of the chromatic space, in particular, to the color direction of the test [14]. However, this is not what the results of Gegenfurtner and Kiper suggest. When the noise was varied and the test direction was fixed, the threshold elevation of their Gabor stimuli always fell well within the cosine prediction made by the multiple-broadly-tuned mechanisms hypothesis (if the test is detected by a single one of these mechanisms and if the noises have constant power, then the threshold elevations should be proportional to the cosine of the angle between noise and test direction). Gegenfurtner and Kiper's results are consistent with the situation we have depicted in Fig. 1(c and f).

Although the experiments of the present study were primarily designed to investigate the existence of narrowly-tuned chromatic mechanisms, some of the findings bear on the question of whether there are multiple broadly-tuned higher order chromatic mechanisms as well. Our conclusion is that our results may be accounted for by only two, approximately linear (broadly-tuned) detection mechanisms that can be identified as the RG and the luminance mechanism, consistent with Fig. 1(b and e).

2. Methods

2.1. Mechanisms in cone contrast space

Stimuli are represented in the (ΔL/L, ΔM/M) plane of cone contrast space [15,16]. The contrast of the stimulus, c, is defined as the Euclidean distance of the (ΔL/L, ΔM/M, ΔS/S) point representing the stimulus from the origin:

$$c = [(\Delta L/L)^2 + (\Delta M/M)^2 + (\Delta S/S)^2]^{1/2}$$

In the 3-dimensional cone contrast space, stimuli are represented as vectors whose components are the cone contrasts they produce. A linear mechanism in this space can also be represented as a vector whose components are the cone-contrast weights of the mechanism [6]. For example, the linear RG mechanism can be represented in this space as a vector proportional to $(-1, 1, 0)$ (neglecting small, negative S-cone contribution to this mechanism; [17]).

The response of a linear mechanism $\vec{W} = \{W_L, W_M, W_S\}$ to a stimulus $\vec{x} = \left\{\frac{\Delta L}{L}, \frac{\Delta M}{M}, \frac{\Delta S}{S}\right\}$ is:

$$R = W_L\frac{\Delta L}{L} + W_M\frac{\Delta M}{M} + W_S\frac{\Delta S}{S}$$

which is the same as the dot product of two vectors:

$$R = \vec{W}\cdot\vec{x} = |\vec{W}||\vec{x}|\cos(\alpha)$$

where α is the angle between $\vec{W}$ and $\vec{x}$.

The set of stimuli that do not activate such a linear mechanism (i.e. for which $R = 0$) form a plane called the 'null plane' of the mechanism [18].

This plane is orthogonal to the mechanism vector $\vec{W}$ that gives the most efficient color direction for stimulating the mechanism. A linear mechanism is sensitive to all the stimuli except for the ones in its null plane. The chromatic mechanisms reported by Gegenfurtner and Kiper [1], on the other hand, are mechanisms that are tuned only to a narrow region of the cone contrast space. Narrow tuning cannot be obtained by a linear combination of the cone contrast signals, so these mechanisms are intrinsically non-linear.

In our experiments we do not stimulate the S-cones, and our stimuli and mechanisms may be represented as two-dimensional vectors in the (ΔL/L, ΔM/M) plane. In this plane, vectors that do not yield a response in the mechanism lie in the 'null direction' of the mechanism (the intersection of the null plane with the (ΔL/L, ΔM/M) plane). Lines of constant response, such as a detection contour, are orthogonal to the mechanism vector [6].

2.2. Apparatus

Stimuli were created on a Macintosh computer and displayed on a Nanao monitor by a standard video

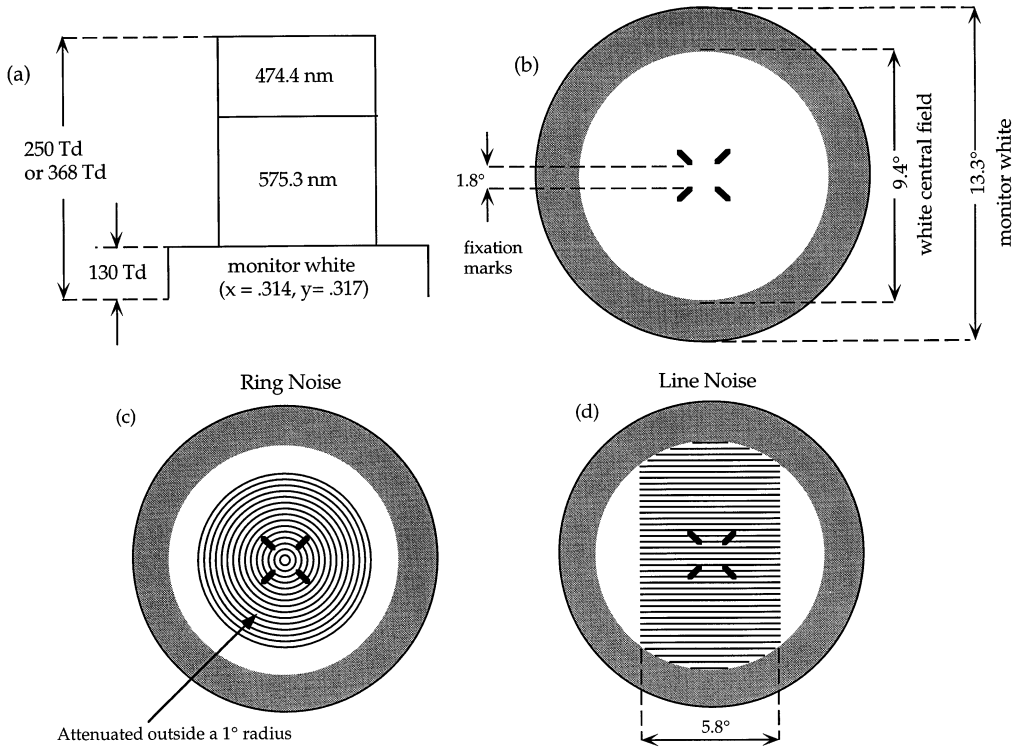

Fig. 2. Display. (a) the adapting field was formed by the superposition of the monitor ($x = 0.314$, $y = 0.317$), with two narrow-band lights in Maxwellian view and metameric to the monitor 'white'. (b) The central field was circular subtending 9.4°, and four fixation marks were used. (c) Ring masking noise filling the central field. Each ring switched randomly between two opposite chromaticities (see Section 2.4). The test was interdigitated between the rings (ring-test-ring-test). The noise contrast was constant within a 1° radius, and then attenuated as a Gaussian (with $\sigma = 1°$). (d) Line masking noise, also half-toned, with uniform contrast.

board with 8-bit digital-to-analog conversion. The mean field formed by the monitor was white ($x = 0.314$, $y = 0.317$), and produced a retinal illuminance of 130 Td (Fig. 2). A circular background field formed by a two-channel Maxwellian view optical system was superposed on the monitor image (Fig. 2b). A grating monochrometer (Jobin-Yvon H-10) in one channel and an interference filter in the other created narrow-band lights with spectral centroids of 474.4 and 575.3 nm, respectively, that were optically combined to create an adapting field with the same chromaticity as the monitor white (Fig. 2a and b). An aperture image formed by two relay lenses created an artificial pupil 2.4 mm in diameter in the observer's pupil plane. The total retinal illuminance in the central 9.4° field was set to 368 Td when the stimuli were Gaussian blobs and to 250 Td when the stimuli were Gabor patches (in order to have sufficient contrast in the Gabors in all color directions). Viewing was foveal and monocular with an achromatizing lens [19] used to correct for chromatic aberration. A bite bar was used to stabilize the observer's head. The observers were instructed to fixate the center of the field, delimited by four fixation marks (Fig. 2b).

2.3. Calibration

Spectroradiometric calibration was performed on the three phosphors of the monitor at 1.05 nm intervals across the visible spectrum. Gamma correction of the monitor output was achieved via software lookup tables.

2.4. Stimuli and noise

The stimuli were either circular Gaussian blobs ($\sigma = 1°$) or horizontal Gabor patches (spatial frequency = 1 cpd, $\sigma = 1°$, in sine phase relative to the center of the envelope), presented as 200 ms flashes against the white background field. The Gabor stimuli are symmetric about the origin in cone contrast space, so each threshold is plotted a second time after reflection about the origin (i.e. half of the plotted Gabor thresholds are redundant—this is not true for the blobs). The masking noise consisted of continuously flickering binary chromatic rings that had their contrast gradually attenuated outside a 1° radius (for the blobs), or 5.8° long horizontal lines (primarily for the Gabor patches), whose

chromaticities were also symmetric about the origin (Fig. 2c and d).

For example, with masking noise of maximum contrast along the 135°/315° direction, each noise ring or line switched randomly and independently from ($\Delta L/L = -0.018$, $\Delta M/M = 0.018$) to ($\Delta L/L = 0.018$, $\Delta M/M = -0.018$). Binary noise was used in order to maximize the noise power. The width of the rings or lines was 2.64 min of arc and the space between them was also 2.64 min of arc. The temporal frequency was 16.8 Hz and the noise was continuously modulated on the display during the entire experimental run. The test was always created in the gaps between the noise rings or lines; the noise pixels were set to the mean field in the no-noise conditions. Given the low spatial resolution of the chromatic mechanisms, the high spatial frequency components created by this half-toning procedure were not visible in the chromatically-detected tests but were occasionally seen for the tests near 45 or 225°.

In order to facilitate comparison with other experiments that did not use half-toned stimuli, all the reported contrast values (test thresholds and noise contrasts) are half the peak contrast of the nominal stimulus profile. Control experiments using direct comparisons of half- and full-toned test stimuli show that this correction is accurate.

2.5. Procedure

Detection thresholds were determined with a 2AFC, adaptive staircase procedure. Observers adapted to the white background field for 2 min before each run of 100 trials. In the noise conditions the subject adapted to the background plus noise. Chromaticities were not intermixed: only a single test color direction (and noise color direction in masking conditions) were used in a run. Each trial consisted of two 200 ms intervals signaled by tones and separated by 400 ms. The observer initiated each trial and received feedback after each response. The stimulus contrast was decreased by 0.1 log units after three consecutive correct responses and increased by the same amount after one incorrect response. Weibull functions were fit to the frequency-of-seeing data using a maximum likelihood method [20] to estimate two parameters of the psychometric function for each stimulus: a threshold estimate corresponding to a detection rate of 82% and an estimate of the psychometric slope. The figures show mean and S.E., both based upon three estimates obtained from three independent runs (i.e. S.E. are based upon between-run variability).

Three practiced observers participated in the experiments: one of the authors (FG) and two undergraduate students (WL) and (PK). All had normal color vision as assessed by the FM-100 test.

3. Results

3.1. Model fits

As will be shown, the general pattern of our results do not show evidence for either a line-element detection model (Fig. 1a and d) or for many, narrowly tuned, detection-mechanisms (Fig. 1c and f) in the ($\Delta L/L$, $\Delta M/M$) plane. The results are consistent with two linear detection mechanisms that can be identified as the opponent RG and the non-opponent luminance mechanism as in Fig. 1b and e. The threshold contours were fit by assuming a two-mechanism detection model and the following summation rule:

$$\left[\frac{1}{T_{RG}}\left(W_{RG,L}\frac{\Delta L}{L}+W_{RG,M}\frac{\Delta M}{M}\right)\right]^{\beta} + \left[\frac{1}{T_{LUM}}\left(W_{Lum,L}\frac{\Delta L}{L}+W_{Lum,M}\frac{\Delta M}{M}\right)\right]^{\beta}=1 \quad (1)$$

where ($W_{RG,L}$, $W_{RG,M}$, $W_{Lum,L}$, $W_{Lum,M}$, T_{RG}, T_{Lum}) are free parameters and β is the summation exponent, assumed to be equal to four [4,5].

We report model fits either by giving the weights (W_L, W_M) for a particular mechanism, or by $\tan^{-1}(W_M/W_L)$, which is the polar angle of the 'mechanism vector' [6] in the ($\Delta L/L$, $\Delta M/M$) plane. For example, the fact that most of the data in Fig. 3 lie on lines of unit slope suggests there is a mechanism with weight $W_M \approx -W_L$ and a mechanism direction near 135°/315°.

Eskew et al. [6] collected estimates of cone weights for the opponent RG mechanism across several studies in the literature and found a very good agreement across subjects, stimuli and experimental conditions. The average L- and M-cone weights reported in their study are -0.70 (S.D. = 0.021) and 0.72 (S.D. = 0.024), respectively, corresponding to a mechanism oriented at 134°/314°. The estimates for the L- and M-contrast weights of the luminance mechanism were much less certain across subjects and experimental conditions. For the mean L- and M-contrast weights of the luminance mechanism they found 0.78 (S.D. = 0.28) and 0.37 (S.D. = 0.45), respectively.

In the two-mechanism fits plotted in our figures, we constrained the red–green contrast weights ($W_{RG,L}$, $W_{RG,M}$) to be (-0.70, 0.72) as in ref. [6] and left the cone weights of the luminance mechanism ($W_{Lum,L}$, $W_{Lum,M}$) and the mechanisms thresholds T_{RG} and T_{LUM} as free parameters. The best opponent mechanism fit (obtained when we do not constrain $W_{RG,L}$ and $W_{RG,M}$) is almost always close to (134°/314°). In no case did we find a significant difference between the best two-mechanism fit (according to Eq. (1) with six free parameters) and the two-mechanism fit with the opponent mechanism constrained at (-0.70, 0.72), according to the

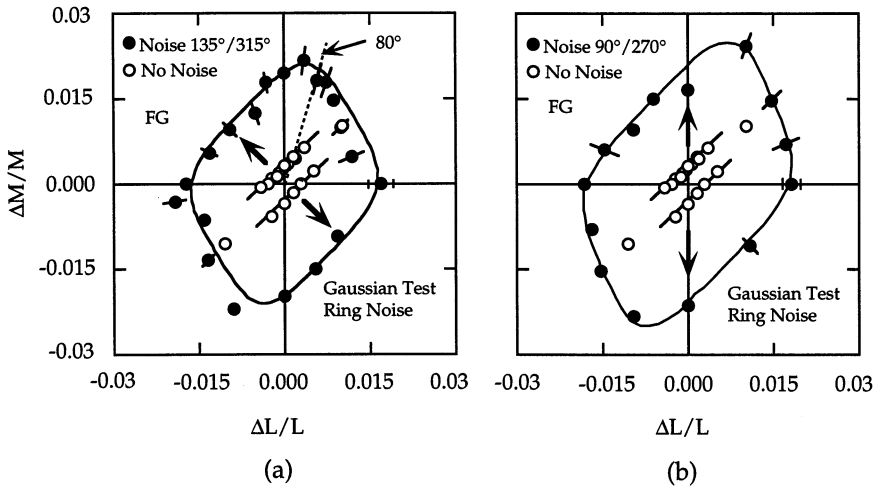

Fig. 3. Threshold contours for Gaussian tests. The arrows represent the direction of the masking noise. Filled symbols represent thresholds after the addition of the ring noise (Fig. 2c), open symbols represent the thresholds in the no-noise condition. The mean retinal illuminance of the field was 368 Td. (a) The chromaticity of the noise was along the 135°/315° direction (contrast = 0.025). (b) The chromaticity of the noise was along the 90°/270° direction (M-cone noise, contrast = 0.040). The solid line is the two-mechanism fit with the opponent mechanism fixed at 134°/314° (see text). The unconstrained two-mechanism fit is (135°/315°, 31°/211°) for (a) and (130°/310°, 20°/200°) for (b).

F-statistic based on the ratio of the two reduced χ^2 s. In the figure legends we report the values of the best two-mechanism fit (with no constraint) for comparison.

The unmasked data (open symbols, Figs. 3, 5 and 7) provide no useful information about the cone weights in the luminance mechanism, since only the thresholds at 45 and 225° are apparently luminance-detected [6,21,22]. For this reason we do not plot the fit of Eq. (1) to the unmasked data, but instead draw lines of unit slope through the RG-detected points, by eye. Table 1 shows the relative RG cone weights obtained when Eq. (1) was fit to the unmasked data, with all the parameters free to vary. In all cases, the relative RG weights are close to the value $W_{RG,M}/W_{RG,L} = -1.03$ predicted from the mean weights $W_{RG,L} = -0.70$ and $W_{RG,M} = 0.72$ that were used to draw the contour on the masked data.

We also fit our thresholds with a three-detection mechanism model. While a three-mechanism fit accounts for more of the variance in the data (smaller χ^2), in no case did we find it to be significantly better than the simple two-mechanism model. In Section 4 we will comment further on this point.

Table 1
RG weights for unmasked data

Observer	Data	$W_{RG,M}/W_{RG,L}$	Test
FG	Fig. 3a and b	−1.03	Blob
WL	Fig. 5a and b	−1.03	Gabor
FG	Fig. 7a	−0.93	Gabor
WL	Fig. 7b	−0.95	Gabor
PK	Fig. 7c	−0.90	Gabor

3.2. Gaussian tests: constant ring-noise direction, variable test direction

Fig. 3(a) shows the threshold contour for Gaussian blobs with and without ring noise, the chromaticity of which varied along the 135°/315° direction. Almost all the stimuli are affected by this noise. The only stimuli not affected are those at 45 and 225° (Fig. 1b and e). This pattern is not consistent with the predictions made by the single mechanism model schematized in Fig. 1a and d. The shape of the detection contour in the presence of noise is also not consistent with the shape expected if detection were mediated by many narrowly-tuned detection mechanisms as described in Fig. 1e and f.

Consider the 80° test direction (Fig. 3a, dotted line). Without noise, this test angle appeared green at threshold. In the presence of the noise, however, this same 80° test angle appeared achromatic at threshold. This fact suggests that the noise is masking an opponent linear 'red–green' mechanism while leaving a second, non-opponent 'luminance' mechanism relatively unaffected. This non-opponent mechanism takes over detection of some stimuli, such as, for example, the test at 80°, when the opponent mechanism is sufficiently masked. The two-mechanism fit yields a non-opponent mechanism of ($W_{Lum,L} = 0.87$, $W_{Lum,M} = 0.5$), i.e. at about 30°/210°.

For noises that are larger than the intrinsic noisiness of the mechanism, masking of chromatic thresholds should be proportional to the contrast of the external noise applied to the mechanism [23]. In this case, that means that threshold elevations should be proportional to the projection of the noise vector onto the RG

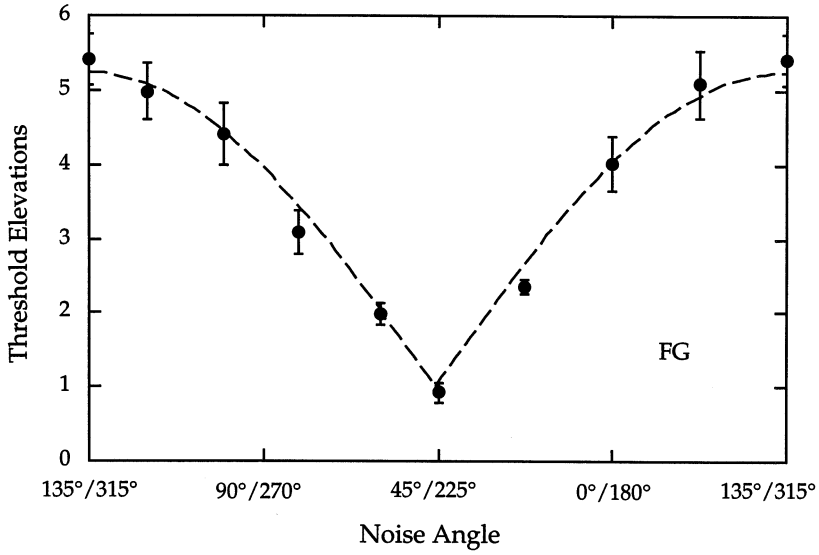

Fig. 4. Spectral tuning of the mechanism detecting the test at 120°. The field was 368 Td, the Gaussian test was fixed at 120° (the approximate equiluminant direction for FG), and the color angle of the ring noise in the (ΔL/L, ΔM/M) plane is shown on the horizontal axis. The contrast of the noise was kept fixed at 0.025. The vertical axis represents test threshold normalized to the unmasked threshold. The dotted line is the best fitting $1+\alpha\,|\cos(\text{Noise Angle}-\gamma)|$ curve (two-parameter fit in α and γ). The best-fit parameter values are: $\alpha=4.2$ and $\gamma=-44.3°$. The null direction for the mechanism detecting the stimulus is 45.7°/225.7°. Masking follows the prediction for a single detection mechanism with a mechanism vector at 135.7°/315.7° in this plane. Error bars were obtained using the formula for the propagation of error [27].

mechanism direction, at about 134°/314°. Noise of constant contrast at other angles should produce less masking of the chromatic threshold and perhaps introduce more masking of the achromatically-detected tests.

Fig. 3(b) shows results with pure M-cone (90°/270°) noise. The noise was set to the maximum possible contrast that we could obtain in that direction. The projection of the maximal 90°/270° noise on the 134°/314° mechanism direction is only about 15% higher than the peak noise contrast when the noise was modulated along 135°/315°. Therefore, the effect of this M-cone noise on the chromatically-detected stimuli should be similar to that in Fig. 3(a), and indeed it is. Note that the luminance thresholds are also slightly elevated, presumably because the M-cone noise has enough of a luminance component to mask the luminance mechanism slightly. The best non-opponent mechanism fit was found at ($W_{\text{Lum,L}}=0.92$, $W_{\text{Lum,M}}=0.39$), i.e. at about 23°/203°.

The results in Fig. 3(b) also seem to be inconsistent with the existence of additional (>2) broadly-tuned higher-order mechanisms. If, for example, the L-cone test were detected by linear mechanisms tuned to the L-cone axis or to a nearby axis, then the M-cone noise, which is 90° away, should have little or no effect on the detection of the L-cone stimulus. This is clearly not true: the elevations are approximately the same for the L- and M-tests and all the stimuli in between.

The model fits show that the luminance mechanism vector is not orthogonal to the chromatic RG direction at 134°/314°. We might, therefore, be surprised that noise at 135°/315° has almost no effect on the tests at 45 and 225° (Fig. 3a). This is not a real inconsistency. To be effective, the masking noise must exceed the intrinsic noise of the mechanism itself (the 'equivalent input noise'; [23]). For example, if we assume that the luminance direction is at about 26°/206° (the average of the two luminance directions revealed by Fig. 3a and b), the projection of the noise at 90°/270° (peak contrast $=0.040$) on the luminance mechanism is $(0.040)\times\cos(90-26°)=0.017$. The projection of the 135°/ 315° noise (peak contrast $=0.025$) on the luminance direction is, instead, $(0.025)\times\cos(135-206°)=0.008$, about half as much. Therefore, the luminance component of the 135°/315° noise is likely to be less than the intrinsic noise of the luminance mechanism, which is why such noise has almost no effect on the 45 and 225° tests.

3.3. Gaussian tests: constant test direction, variable ring-noise direction

In this experiment the Gaussian test was fixed at 120° and threshold elevations for this approximately-equiluminant test were measured as a function of noise angle. The contrast of the noise at each angle was 0.025. Assuming that we are operating in the linear range of the response function of this opponent chromatic mechanism (i.e. 0.025 is substantially greater than the equivalent input noise), the threshold elevations should be proportional to the absolute value of the cosine of the angular difference between the noise direction and the

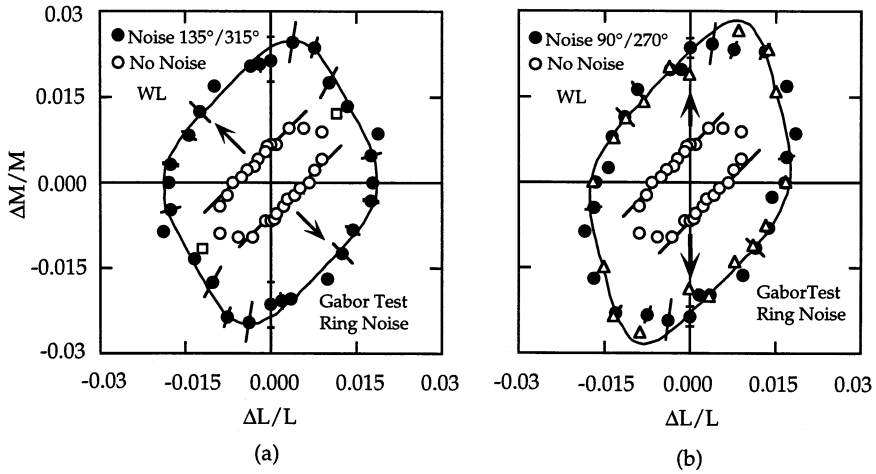

Fig. 5. Threshold contours for Gabor tests after adding chromatic ring noise (Fig. 2c) for observer WL (filled symbols). (a) Noise chromaticity at 135°/315° (contrast = 0.038), (b) Noise chromaticity at 90°/270° (contrast = 0.060). The solid lines are the two-mechanism fit with the opponent mechanism fixed at 134°/314° (see text). The unconstrained two-mechanism fits are: (a) (137°/317°, 30°/210°) and (b) (136°/316°,18°/198°). The empty squares in (a) are the no-noise thresholds from Fig. 7b. The empty triangles in (b) are replications. The arrows represent the direction of the masking noise. The retinal illuminance was 250 Td.

mechanism direction. As shown in Fig. 4, the threshold elevations do follow a |cosine| function, consistent with the test being detected by a single linear mechanism that has a mechanism direction near 135°/315° and a null direction near 45°/225°. Note that this chromatic null direction at about 45°/225° is not the luminance mechanism direction, because the two detection mechanisms are not orthogonal [6], at least for this observer under these conditions.

Like the results in Fig. 3(b), these results are not consistent with detection by a linear higher-order chromatic mechanism that is tuned to the direction of the test. The null direction of that mechanism would be 30° (120 − 90°), not the 45° null in Fig. 4.

The results obtained so far require only two detection mechanisms in this plane. They are in agreement with both Krauskopf et al. [11] and Gegenfurtner and Kiper [1], who also found evidence for just two detection mechanisms when stimuli with a dc component are used. In the next experiments we used horizontal sine phase Gabors (dc = 0) embedded in masking noise.

3.4. Gabor tests: constant ring-noise direction, variable test direction

Thresholds for the detection of Gabor patches embedded in 135°/315° and 90°/270° ring-noises were measured for a second observer (WL). The results (Fig. 5) do not show narrowly-selective masking at the noise-direction, suggesting that detection of Gabor tests is not mediated by chromatic mechanisms narrowly tuned in the chromatic space (the empty triangles in Fig. 5(b) are a replication). The masking in this case is less powerful than with the Gaussian blobs. This is not surprising since most of the energy of the test is now along the horizontal spatial orientation while the masking rings have their energy spread among all spatial orientations.

In Fig. 5(a) the observer appears to have a little elevation along the 45°/225° direction. This might be due to some masking produced by the 135°/315° noise on his luminance mechanism or, more likely, to a no-noise threshold in this direction that was unusually low (the empty squares at 45 and 225° are replotted from the same conditions in Fig. 7b). In any case, the elevation of this test is significantly smaller than the elevations of the chromatically detected tests (the elevation of the test at 135°/315°, for example, is 4.6 while the elevation of the test [open circle] at 45°/225° is only 1.5).

With the noise at 135°/315° (Fig. 5a), the best luminance mechanism fit is at about 28°/208°, while with noise at 90°/270° (Fig. 5b), the best luminance mechanism fit is at about 15°/195°. The luminance mechanism fit to Fig. 5(a and b) suggests that for this observer, as for FG (Fig. 3), the L-cones contribute more than the M-cones to the luminance signal in contrast terms.

3.5. Gabor tests: constant line-noise, variable test direction

In this experiment we used horizontal lines of various chromaticities to mask the Gabor tests. This masking pattern should produce more masking than the rings since most of its energy is concentrated along the horizontal spatial orientation, matching the test. We used both M-cone (90°/270°) noise and L-cone (0°/180°) noise. The peak cone contrast produced by these noises was the same (0.049), meaning that their masking power for the opponent RG mechanism was also approximately the same (Fig. 6). In comparison, the

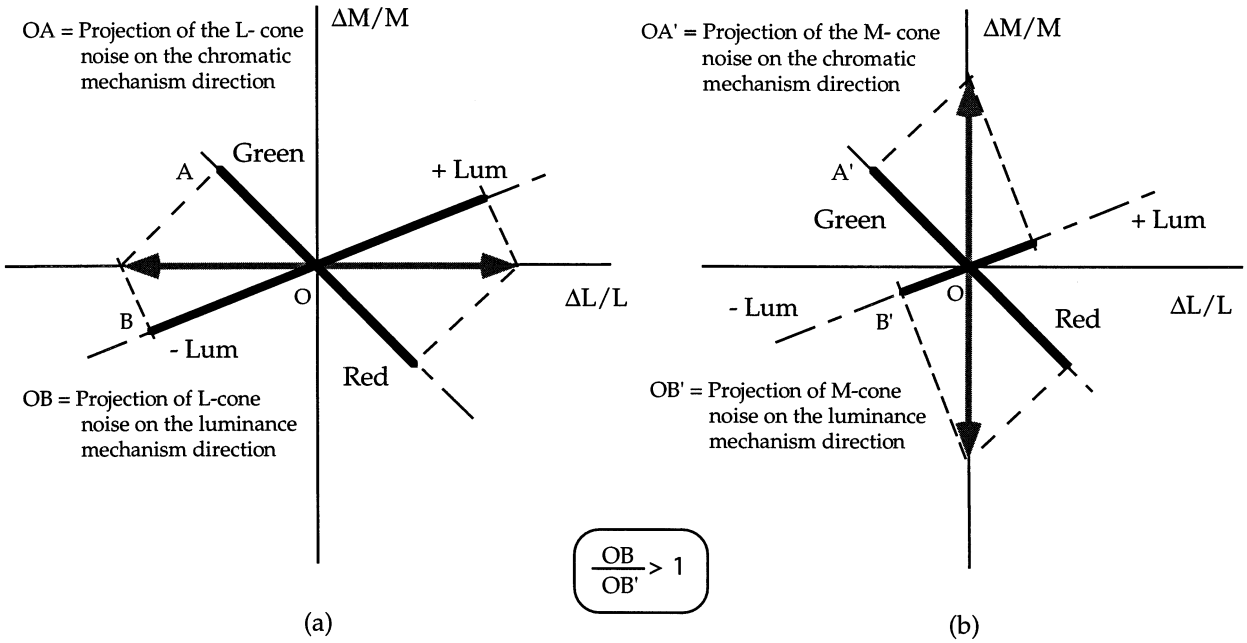

Fig. 6. Possible effects of the L-cone noise and M-cone noise on the RG and luminance mechanisms. The L-cone (a) and M-cone (b) noises have nearly the same projection, and thus the same masking effect, on the RG mechanism. If the luminance mechanism direction is at an angle less than 45°, then the L-cone noise (a) has a larger masking effect on the luminance mechanism than the M-cone noise (b).

effect of these noises on the luminance mechanism is potentially very different. For example, the results of the preceding experiments suggested that the luminance mechanism has a larger L-cone contrast weight. This means that the L-cone noise should produce more masking of the luminance mechanism than the M-cone noise (Fig. 6). The data for a third observer (PK) are also presented.

As shown in Fig. 7, L-cone and M-cone noises mask the chromatically-detected thresholds (those near 135°/315°) to the same degree for all three observers. However, observer differences appear when luminance-detected tests are considered. For FG, the L-cone noise produces a 3.3-fold elevation of the luminance-detected test at 45°, whereas the elevation produced by the M-cone noise is 1.3. The ratio of the two elevations, which is an estimate of the relative effectiveness of the two noises on the luminance mechanism, is 2.5. This would be consistent with a luminance mechanism direction of about 24°/204°. The two best-fitting luminance mechanisms for FG are at 22°/202° (with M-cone noise) and 25°/205° (with L-cone noise).

For WL (Fig. 7b), the luminance portion of the contour is inconsistent with the earlier result. While Fig. 5 indicates that WL's luminance mechanism is similar to FG's in weighting the L cones more than the M cones, Fig. 7(b) strongly suggests approximately equal weights for WL because the thresholds at 45° are almost identical for both L-cone and M-cone noise. The best-fitting luminance mechanisms are 39°/219° for M-cone noise and 48°/228° for L-cone noise. We cannot explain this partial discrepancy between Figs. 5 and 7, but it does not affect our main conclusion: these results are not consistent with multiple, narrowly-tuned detection mechanisms in this plane.

Fig. 7(c) reports the results for observer PK. As the no-noise data show, this observer was less sensitive than the other two and, to allow a reliable estimate of the contrast thresholds in the noise conditions, we decreased the peak noise contrast to 0.030. As for WL, the L- and M-cone noises have almost the same effect on all tests, including the test at 45°, suggesting a luminance mechanism that weights the L- and M-cones approximately equally. The best luminance mechanism fits are: 46°/226°, with M-cone noise, and 44°/224° with L-cone noise.

3.6. Effects of L- and M-cone ring noise masks on Gabor tests

A detection contour for horizontal Gabors embedded in ring noise whose chromaticity was modulated along the L- and M-cone axes was obtained for observer FG. Fig. 8 shows the detection thresholds. L-cone ring noise seems to mask the chromatically-detected tests less than M-cone ring noise. This result is puzzling since L- and M-cones seem to contribute about equally to the RG mechanism, and as shown in Fig. 7, L- and M-cone line noises mask the chromatically-detected stimuli equally.

Fig. 9 shows the thresholds for an approximately-equiluminant Gabor test (120°) embedded in line and ring noise as a function of noise energy level. The line

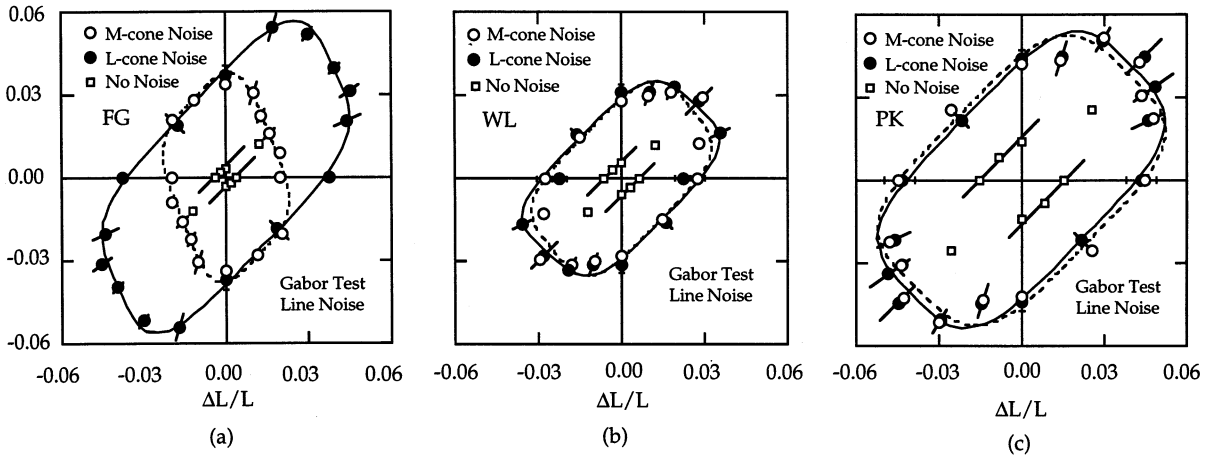

Fig. 7. Threshold contour for Gabor tests after adding L-cone line noise (filled circles) and M-cone line noise (open circles). The cone contrast for both L- and M-cone noises was 0.049 for FG and WL, 0.030 for PK. The retinal illuminance was 250 Td. For observer WL the thresholds at 45° in both L- and M-cone noise conditions are identical and have been slightly displaced in the graph to make them visible. The continuous solid curves in (a), (b), and (c) are the two-mechanism fits with the opponent mechanism fixed at 134°/314° for L-cone noise. The dashed lines are the same fits for M-cone noise (see text). The unconstrained two-mechanism fits are: (a) L-cone noise: (135°/315°, 27°/207°), M-cone noise: (120°/300°, 18°/198°), (b) L-cone noise: (148°/328°, 81°/261°), M-cone noise: (113°/293°, 172°/352°), (c) L-cone noise: (120°/300°, 3°/183°), M -cone noise: (115°/295°, 2°/182°).

noise masks the equiluminant Gabor test more than the ring noise does, but while the L- and M-cone line noises have essentially the same masking effect, L-cone ring noise masks less than M-cone ring noise.

This apparently puzzling result turns out to have a very simple explanation. Unlike the line noise, the ring noise is always centered on the test, potentially helping the observer to localize its position (Fig. 2). Furthermore, for observer FG the L-cone noise has a higher luminance contrast than M-cone noise, given that his luminance mechanism weights the L-cones more than the M-cones (Fig. 6). Therefore, the flickering rings modulated along the L-cone direction can demarcate the test area better than the rings modulated along the M-cone direction, because their luminance contrast is higher; the chromatic contrast produced by L- and M-ring noise is the same.

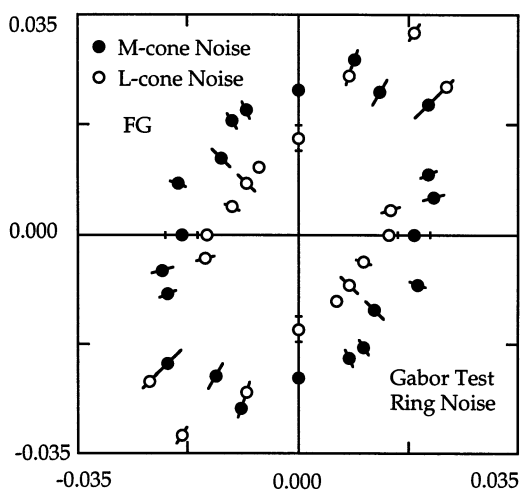

Fig. 8. Thresholds for Gabor tests embedded in L- and M-cone ring noise. Retinal illuminance was 292 Td, and the contrast of both the L- and M-ring noise was 0.049. M-cone ring noise has a larger masking effect on the RG mechanism than L-cone ring noise.

We tested this idea by measuring the thresholds for the detection of an L-cone, an M-cone, and an approximately equiluminant Gabor test, embedded in ring and line noise that surrounded the test but did not cover it. The tests were presented inside an approximately 2° circular window and the surrounding masking noises were rings and lines modulated along the L- and M-cone direction (Fig. 10a and c). If our conjecture were correct we should find a difference between the L- and M-cone ring noises: L-cone ring noise should help the observer to localize the test area better than M-cone ring noise. We would also expect the line noise to produce the same effect: the end points of the lines around the window produce a luminance contrast with the background that is higher for the L-cone noise than for the M-cone noise. This effect should, however, disappear if we add a black ring around the window because, in this case, the test region is clearly demarcated regardless the chromaticity of the surrounding noise.

As predicted, the chromaticity of the noise differentially masks the tests in both cases (Fig. 10b and d), but when the black ring is added to the circular window to demarcate the test region (Fig. 11a and c), the effect disappears (Fig. 11b and d).

This effect is a direct consequence of the fact that, for this observer, the luminance mechanism direction is closer to the L-cone axis, i.e. L-cones contribute more than M-cones to luminance.

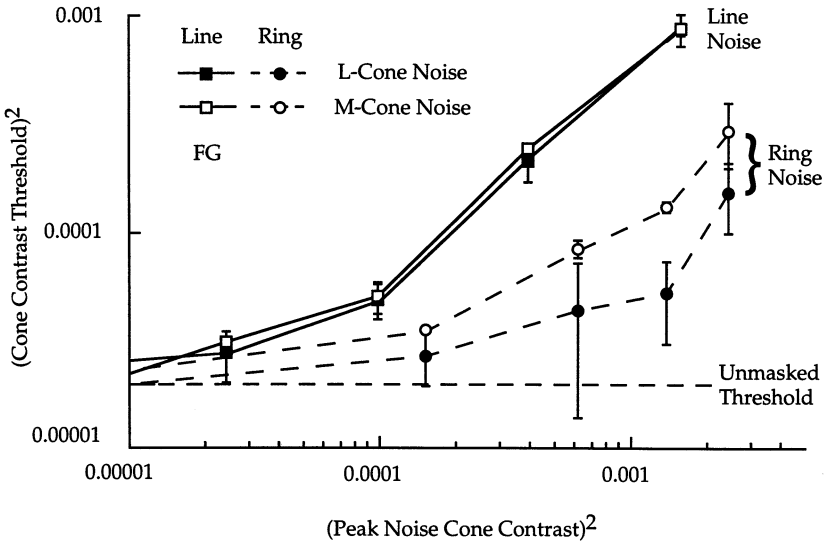

Fig. 9. Thresholds for the detection of an approximately-equiluminant test (120°) as a function of the energy level of the noise. Two spatial configurations (lines and rings, Fig. 2), and two chromaticities (L and M) of the noise are shown. Error bars were obtained using the formula for the propagation of error [27].

4. Discussion

The main result of our masking experiments is that thresholds in the (ΔL/L, ΔM/M) plane are not maximally elevated along the direction of the masking noise, whether or not the test stimuli have a non-zero spatial average. These results suggest that detection is mediated by the activity of only two mechanisms in this plane of color space: one, an opponent mechanism that generates a signal proportional to the weighted difference of the L- and M-cone contrast signals; the second, a non-opponent mechanism that generates a signal proportional to a weighted sum of L- and M-cone signals.

The tests near 45 and 225° activate the yellow-blue mechanism too, and this could be the mechanism that is responsible for their detection. Although possible, this seems unlikely since the observers reported that the stimuli in that direction looked achromatic at threshold. Furthermore, there is psychophysical evidence suggesting that the YB mechanism is less sensitive than the luminance mechanism for spatio-temporal conditions like those used here [4].

Another interesting finding is that the masking revealed part of the achromatic flank of the detection contour that is normally invisible, given the much higher sensitivity of the chromatic mechanism. For observer FG, the average luminance direction is 25°/205°, corresponding to an L:M cone contrast weight ratio of about 2.2:1. For observer WL, the luminance direction is less certain; there is an apparent discrepancy between Figs. 5 and 7, as already discussed. Averaging over these results, the luminance direction for WL is 33°/213° corresponding to an L:M ratio of about 1.6:1. Previous psychophysical studies have also found observer differences in the cone contrast weights for the luminance detection mechanism [6].

Our results are consistent with Krauskopf et al. [11] and Sankeralli and Mullen [9], but are partially at odds with the data obtained by Gegenfurtner and Kiper [1], whose masking study was in many ways similar to ours. Gegenfurtner and Kiper speculated that stimuli containing a dc component might be more effective stimuli for LGN cells than for cortical cells and might, therefore, be less effective at tapping the activity of the narrowly-tuned color mechanisms. We find no qualitative difference between our zero dc and non-zero dc stimuli.

Another important issue is whether detection in this plane might be mediated by multiple, broadly-tuned, linear higher-order mechanisms. Masking studies in the equiluminant plane by D'Zmura and Knoblauch [14] are consistent with this hypothesis. Several other psychophysical studies involving more 'high level' tasks like color appearance, visual search and color constancy [10,13,24] also suggest that the mechanisms mediating these tasks are linear and tuned to various chromaticities of the chromatic space. There could be many such mechanisms 'hard-wired' to provide a very fine color representation; alternatively, these mechanisms could be 'soft-wired', resulting from an adaptive process that rotates the mechanisms to optimally detect a given test (one possible adaptive process of this kind has been used by Atick et al. [25], to explain the color appearance data of Webster and Mollon [26]). The question is whether mechanisms of either kind might be able to explain our data. We do not think so. First of all we have shown that the data can be easily fitted by

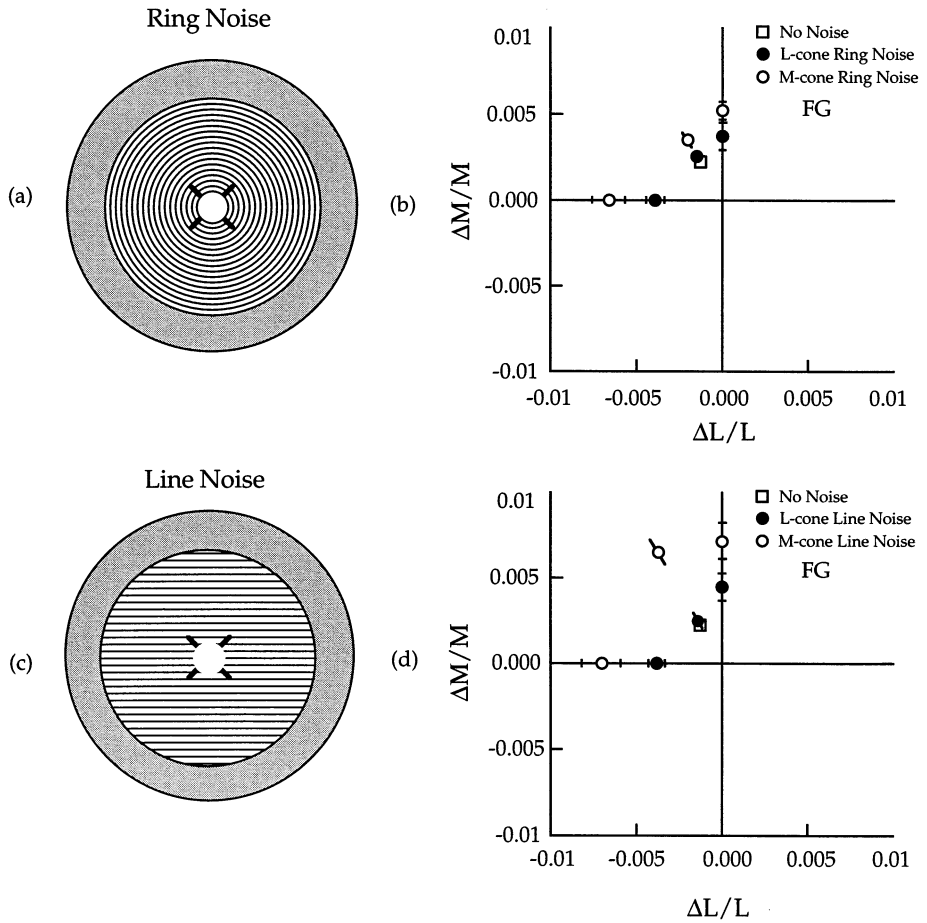

Fig. 10. Effects of surrounding L- and M-ring and line noises on chromatic detection. The tests were presented within an approximately 2° window surrounded by the noise. The window causes L- and M-noises to differ for both rings and lines. Retinal illuminance was 250 Td; the contrast of both noises was 0.049. Unlike in the earlier experiments, both noises filled the full field at constant contrast, excepting only the central window.

a simple two-mechanism model (an opponent and a non-opponent) model. Furthermore, with both Gaussian blobs and Gabor patches, noise along one of the cone axis had the same masking effect on test stimuli along that cone axis as along the orthogonal one (Fig. 3b, Fig. 7a, b and c). In addition, the null direction for the mechanism detecting a Gaussian blob at 120° is not 30 but 45° (Fig. 4), consistent with an opponent mechanism at about 135°/315°.

However, the nearly-vertical alignment of the thresholds near the horizontal axis in Fig. 5 might be taken as evidence of intrusion of a third linear mechanism that is L-cone dominated. This seems to be particularly the case for the threshold contour of Fig. 5(b) when the noise is at 90°/ 270°. We compared the best two- and three-mechanism model fits to the data in Fig. 5 to determine if a third mechanism were needed. With noise at 135°/315°, the three-mechanism model accounts for more variance ($\chi^2 = 0.045$ for the two-mechanism fit and $\chi^2 = 0.035$ for the three-mechanism fit) but is not significantly better, given the reduced degrees of freedom ($F(8, 5) = 0.8$, $P = 0.37$). With noise at 90°/ 270°, the three-mechanism model accounts for much more of the variance ($\chi^2 = 0.024$ vs $\chi^2 = 0.067$ for the two-mechanism fit). However, this difference is still not significant at conventional alpha levels ($F(8, 5) = 1.74$, $P = 0.28$). Thus, the two-mechanism fit and the three-mechanism fit to Fig. 5(b) are not distinguishable on statistical grounds. In fact, the three-mechanism model fails to be significantly better than either the constrained or unconstrained two-mechanism models in every data set from Figs. 3, 5 and 7. Given that the fit to a threshold contour can always be improved by arbitrarily increasing the number of detection mechanisms in the model, we hold to the more conservative two-mechanism model, the one that works well to explain many previous results [6].

Acknowledgements

Supported by NIH EY09712. We thank K. Knoblauch, J. McLellan, M. Sankeralli and C. Stromeyer for helpful discussions and suggestions, and W. Lee and P. Kortick for serving as observers.

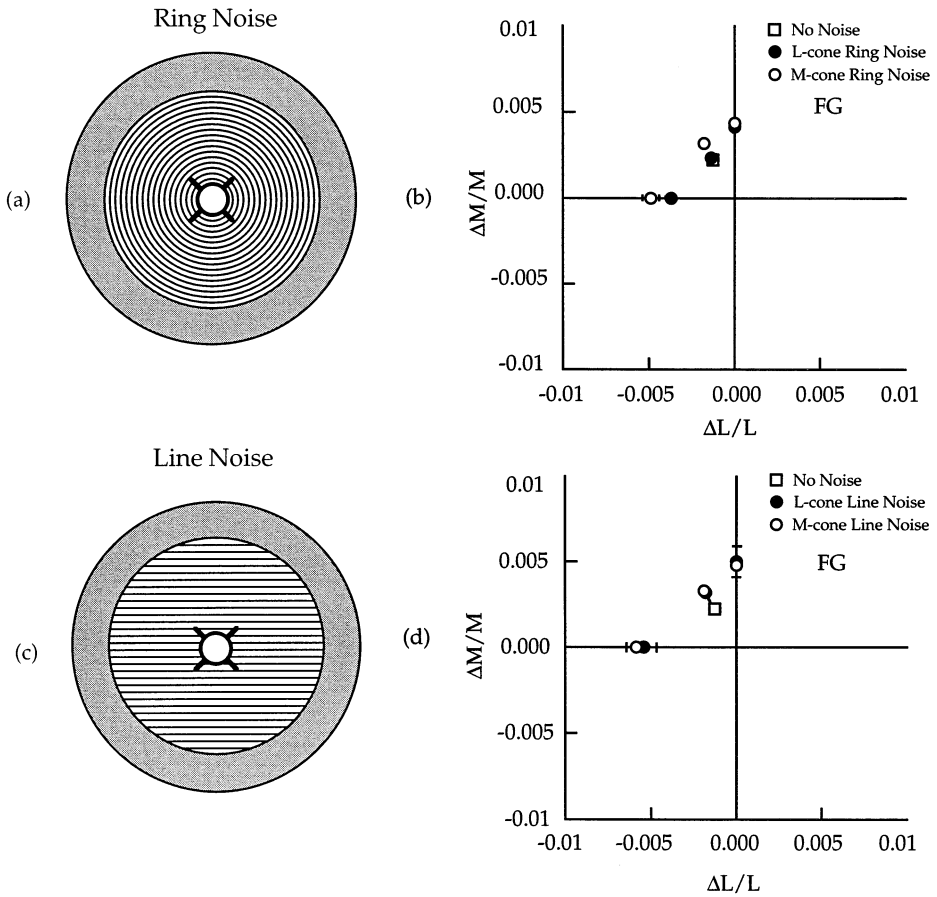

Fig. 11. Effects of surrounding L- and M-ring and line noise on chromatic detection when the test area is always demarcated by a black ring. The ring reduces the M-noise thresholds, eliminating the difference between the two noise chromaticities. Retinal illuminance was 250 Td; the contrast of both noises was 0.049. Noises as in Fig. 10.

References

[1] Gegenfurtner KR, Kiper DC. Contrast detection in luminance and chromatic noise. J Opt Soc Am A 1992;9:1880–8.

[2] Boynton RM, Kambe N. Chromatic difference steps of moderate size measured along theoretically critical axes. Color Res Appl 1980;5:13–23.

[3] Chaparro A, Stromeyer CF III, Chen G, Kronauer RE. Human cones appear to adapt at low light levels: measurements on the red-green detection mechanism. Vis Res 1995;35:3103–18.

[4] Cole GR, Hine T, McIlhagga W. Detection mechanisms in L-, M-, and S-cone contrast space. J Opt Soc Am A 1993;10:38–51.

[5] Cole GR, Hine TJ, McIlhagga W. Estimation of linear detection mechanisms for stimuli of medium spatial frequency. Vis Res 1994;34:1267–78.

[6] Eskew RT Jr, McLellan JS, Giulianini F. Chromatic detection and discrimination. In: Gegenfurtner KR, Sharpe LT, editors. Color Vision: From Molecular Genetics to Perception. Cambridge: Cambridge University Press, 1998.

[7] Guth SL. Model for color vision and light adaptation. J Opt Soc Am A 1991;8:976–93.

[8] Sankeralli MJ, Mullen KT. Estimation of the L-, M-, and S-cone weights of the postreceptoral detection mechanisms. J Opt Soc Am A 1996;13:906–15.

[9] Sankeralli MJ, Mullen KT. Detection mechanism directions revealed by noise masking in a three dimensional cone contrast space. Invest Ophthalmol Vis Sci 1996;37:S427.

[10] D'Zmura M. Color in visual search. Vis Res 1991;31:951–66.

[11] Krauskopf J, Williams DR, Heeley DW. Cardinal directions of color space. Vis Res 1982;22:1123–31.

[12] Krauskopf J, Williams DR, Mandler MB, Brown AM. Higher order color mechanisms. Vis Res 1986;26:23–32.

[13] Webster MA, Mollon JD. The influence of contrast adaptation on color appearance. Vis Res 1994;34:1993–2020.

[14] D'Zmura M and Knoblauch K. Spectral bandwidths for the detection of color. Vis Res 1998 (in press).

[15] Noorlander C, Koenderink JJ. Spatial and temporal discrimination ellipsoids in color space. J Opt Soc Am A 1983;73:1533–43.

[16] Brainard DH. Appendix, Part IV: Cone contrast and opponent modulation color spaces. In: Kaiser PK, Boynton RM, editors. Human Color Vision. Washington, DC: Optical Society of America, 1996:563–79.

[17] Stromeyer CF III, Chaparro A, Rodriguez C, Chen D, Hu E, Kronauer RE. Short-wave cone signal in the red-green detection mechanism. Vis Res 1998;38:813–26.

[18] Derrington AM, Krauskopf J, Lennie P. Chromatic mechanisms in lateral geniculate nucleus of macaque. J Physiol 1984;357:241–65.

[19] Powell I. Lenses for correcting chromatic aberration of the eye. Appl Opt 1981;20:4152–5.

[20] Watson AB. Probability summation over time. Vis Res 1979;19:515–22.

[21] Cole GR, Stromeyer CF III, Kronauer RE. Visual interactions with luminance and chromatic stimuli. J Opt Soc Am A 1990;7:128–40.

[22] Stromeyer CF III, Cole GR, Kronauer RE. Chromatic suppression of cone inputs to the luminance flicker mechanism. Vis Res 1987;27:1113–37.
[23] Pelli DG. The quantum efficiency of vision. In: Blakemore C, editor. Vision Coding And Efficiency. Cambridge: Cambridge University Press, 1990:3–31.
[24] D'Zmura M, Lennie P. Mechanisms of color constancy. J Opt Soc Am A 1986;3:1662–72.
[25] Atick JJ, Li Z, Redlich AN. What does post-adaptation color appearance reveal about cortical color representation? Vis Res 1993;33:123–9.
[26] Webster MA, Mollon JD. Changes in colour appearance following post-receptoral adaptation. Nature 1991;349:235–8.
[27] Bevington PR. Data Reduction and Error Analysis for the Physical Sciences. New York: McGraw-Hill, 1969.